Marine Geology 398 (2018) 99–111

Contents lists available at ScienceDirect

Marine Geology

journal homepage: www.elsevier.com/locate/margo

Climate and tectonic-driven sedimentary infill of a lagoon as revealed by high resolution seismic and core data (the Nador lagoon, NE Morocco)

O. Raji[a,b,*], L. Dezileau[b], B. Tessier[c], S. Niazi[d], M. Snoussi[d], U. Von Grafenstein[e], A. Poujol[f]

[a] Geology and Sustainable Mining, Mohammed VI Polytechnique Univ., Benguerir, Morocco
[b] Geosciences Montpellier, UMR 5243, CNRS, Montpellier Univ., Montpellier, France
[c] Morphodynamique Continentale et Côtière (UMR M2C), Caen Univ., Caen, France
[d] Department of Earth Sciences, Mohammed V Univ., Rabat, Morocco
[e] Sciences du Climat et de l'Environnement, CNRS/CEA, Saclay, France
[f] Earth Science Building, Geomechanics Group, National Central Univ., Taoyuan, Taiwan

ARTICLE INFO

Keywords:
Mediterranean Sea
Sedimentary fill
Nador lagoon
Morocco
Seismic
Sediment cores
LIA
Tectonic

ABSTRACT

Lagoonal systems are vulnerable environments in the present day context of global climate change. The study of their sedimentary infill is critical to understand marine and continental factors controlling their evolution, and in so doing, evaluate their future behaviour and potential management. In that context, Mediterranean lagoons are particularly important due to their social and economic values. The Nador lagoon, located along the Western Mediterranean coast, is the largest Moroccan lagoon. In order to study its sedimentary infill, very high-resolution seismic reflection data were acquired, providing for the first time an image of the architecture of the infilling Holocene deposits. The combination between sediment core information and seismic data allows the reconstruction of the lagoon history over the last millennium. We demonstrate that the time between the 15th and 19th century has been a key period in the lagoon evolution. Sand bodies of marine origin dominated the sedimentary infill of the lagoon during that time. We propose that this stage of the Nador lagoon, the evolution and infilling is closely linked both to the local tectonic and Little Ice Age climatic contexts. These results are important to understand the mode of evolution of other comparable lagoons along microtidal coasts.

1. Introduction

The Mediterranean coastal lagoons are highly productive with significant ecological, historical, economic, and social relevance. As a consequence, they are subjected to heavy human pressure such as urbanization and pollution (Cañedo-Argüelles et al., 2012). In addition, their coastal setting makes them vulnerable to the global climate change, which strongly affects the land to sea transitional areas (Ferrarin et al., 2014). In recent years, the late Holocene evolution of coastal areas and lagoons has been subject to increasing attention by the scientific community. Indeed, compared to deep marine environments, little attention was paid to coastal archives because they were assumed to poorly preserve environmental changes due to climate or tectonic activities. Since new proxy (geochemistry, biology…etc.) and investigation method (VHR resolution seismic tools) development, coastal systems are subject to more and more studies, mainly to evaluate their past changes and underline their vulnerability to future shifts in sea level and climate. This is critical in the context of environments with high social and economic values.

Very High-Resolution (VHR) seismic data, coupled with sediment cores and dating provide a powerful approach that is now commonly used for Holocene stratigraphic reconstructions (e.g. Chaumillon et al., 2010 for a review of Holocene infills along French coasts). This combined approach is particularly well adapted to examine the infill of coastal lagoons (e.g. Ferrer et al., 2010; Raynal et al., 2010; Zecchin et al., 2014) which constitute about 13% of coastal regions (Barnes, 1980). Lagoons are sheltered from high-energy marine reworking by coastal barriers so that their sedimentary infill represents valuable archives to reconstruct changes of environmental conditions, especially those related to climate and most specifically to storm dynamics - known as - paleo-tempestology (Liu and Fearn, 1993; Donnelly et al., 2004; Dezileau et al., 2011; Sabatier et al., 2012; Kakroodi et al., 2012; Das et al., 2013; Raji et al., 2015; Degeai et al., 2015). The coastal lagoons represent also good archives for the reconstruction of human-induced impacts, mainly hydraulic (Tosi et al., 2009) as well as climate and anthropogenic forcing together (Stefani and Vincenzi, 2005). Tapping into the development of dating technics becoming increasingly precise, these studies have moved towards high-resolution

* Corresponding author at: Geology and Sustainable Mining, Mohammed VI Polytechnique Univ., Benguerir, Morocco.
E-mail address: otmane.raji@um6p.ma (O. Raji).

https://doi.org/10.1016/j.margeo.2018.01.010
Received 8 November 2017; Received in revised form 11 January 2018; Accepted 22 January 2018
Available online 03 February 2018

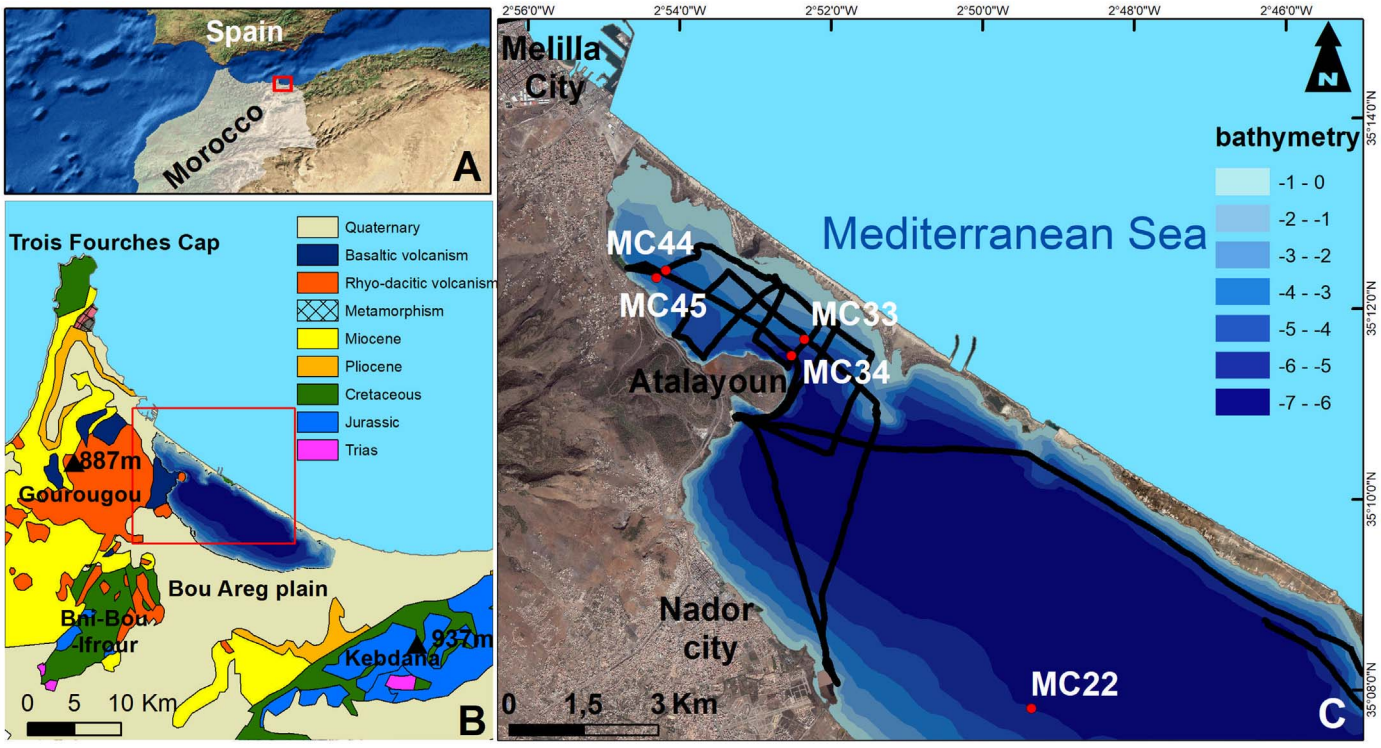

Fig. 1. The Nador lagoon, Morocco. A) General location; B) simplified geological map of the Nador area. The red square indicates the study area; C) bathymetric map of the Nador lagoon (land image from Google Earth) with the position of the very high resolution seismic profiles (black lines) and sediment cores (red spots). (1) The paleo-inlet opened by the 1889 storm event. (For interpretation of the references to colour in this figure legend, the reader is referred to the web version of this article.)

reconstructions and establishing links between large-scale climatic/tectonic forcing factors and local sedimentary events (e.g. Degeai et al., 2015; Dezileau et al., 2011; Donnelly et al., 2004; Nott, 2004). In the context of global warming and related sea-level rise, such studies are appealing for decision-makers in order to build sustainable coastal management scenarios and adaptation of coastal defences (Chaumillon et al., 2017; Goslin and Clemmensen, 2017). However, lagoon sediment archives result from multiple sediment sources (marine, continental and eolian inputs) potentially subject to both climate and tectonic controls. Hence, their study is not an easy task and should take into to account the serious limitations influencing the many proxies that are generally used (Goslin and Clemmensen, 2017) and as such be based on very high resolution multi-proxy analyses (Carvalho do Amaral et al., 2012).

The coastal zone of Nador (southwestern Mediterranean Sea) is characterized by a seven kilometre-wide lagoon (Fig. 1) separated from the sea by an emerged sandy barrier a few hundreds of metres wide. This specific morphology results from a well-known process of shore construction by waves and currents in a microtidal environment (Barusseau et al., 1996). Until now, most studies on this lagoon have focused on the hydrodynamic regime and its impact on recent sedimentation (Bloundi, 2005; Carpio, 1995; Hamoumi, 2012). The few existing studies on its sedimentary infill and past evolution, were all based on short (< 1 m) cores (Irzi, 1987, 2002; Mahjoubi, 2001). In this paper, we present the results of the first seismic survey conducted in the Nador lagoon. The seismic data combined with previously acquired sediment cores are interpreted and used to discuss the evolution of the Nador coastal area during the late Holocene, with the purpose of evaluating their vulnerability with respect to extremes storm surges and earthquake related consequences (tsunamis, liquefaction). The Nador lagoon is a unique lagoon in the southwestern Mediterranean and constitutes a good target for the regional studies of paleo-data compilation and the investigation of the role episodic events can play in lagoonal evolution at millennium to centennial time scale.

2. Location and geological context of the study area

The Nador lagoon, also called Sebkha Bou-Areg or Mar-Chica, is the westernmost lagoon of the Mediterranean basin and moreover is the only lagoon of the Moroccan Mediterranean coast (Fig. 1). With a surface area of 115 km^2, Mar Chica is the largest lagoon of Morocco. The lagoon has an oval shape interrupted in the North by a small peninsula on which rises the Atalayoun hill (112 m), thus dividing the lagoon into two parts (Fig. 1). Its average water depth is 4.8 m, with a maximum depth of 8 m. The Nador lagoon is isolated from the Mediterranean Sea by a 25 km long sandy barrier crossed by an artificial inlet that has been very recently (in 2011) opened and stabilized. The watershed of the lagoon drains an area of 700 km^2. It is composed of several intermittent streams with irregular flow, some of which presently serve as sewerage outflows for urban areas (Irzi, 2002). Around the lagoon, four geological structures can be identified (Fig. 1B): (i) in the northwest, the volcanic massif of Gourougou composed of three Miocene and Pliocene volcanic units: calc-alkaline (9 to 6.6 Ma), shoshonitic (7 to 5.4 Ma) and alkaline (4.7 to 2.6 Ma) rocks (El Azzouzi et al., 1999); (ii) in the west, the massif of Beni Bou Ifrour consists of Jurassic limestones, calcareous sandstones and marls, and of Cretaceous sandy shales and volcano-sedimentary series covered by Miocene detrital sediments. A gypsohaline Triassic formation is also present in the South of the Bni Bou Ifrour (Lebret, 2014); (iii) in the South, the Kebdana massif structured in an east-west strip is mainly composed of Jurassic formations discordantly overlain by Miocene deposits (De Luca, 1978); and (iv) in the southwest, the Bou-Areg Plain consists of very thick Plio-Quaternary formations made of gravels, sands and silts (Guillemin and Houzay, 1982).

In terms of tectonic context, the Nador lagoon is located between two main ~NE-SW structures considered as active during the Neogene (Ait-Brahim et al., 1990; Meghraoui et al., 1996; Morel, 1987; Poujol et al., 2014), i) the linear strike-slip Nekor fault 50 km westward, and ii) the thrust-and-fold Kebdana massif ~10-km south-eastward. Moreover,

there is some geological and seismological evidence showing mainly strike-slip (left-lateral) and transpressionnal structures associated to minor extensional deformation surrounding the Nador lagoon and Melilla region. The compressional fault systems, probably related to the alpine tectonic stage, are delimited by two NE-SW-oriented left-lateral strike-slip faults localized at the foothills of the Kebdana folded massif (belonging to the Anti-Atlas) at south and the Beni Bou Ifrour massif (belonging to the Rif belt) at north (Ait-Brahim et al., 1990; Comas et al., 1999; Morel, 1989; Yahyaoui et al., 1997). The other left-lateral faults mark the contact between the different geological units with the same NE-SW orientations. Finally, N−S trending east-dipping normal faults are localized westward of Melilla and Nador lagoon and crosscut the strike-slip fault, suggesting a present-day control on the subsidence within the Bou Areg plain (Ait-Brahim et al., 1990; Chotin and Brahim, 1988; Louaya and Hamoumi, 2010).

In addition, detailed studies of the Mediterranean marine terraces along the Moroccan shorelines (Guillemin and Houzay, 1982; Meghraoui et al., 1996; Morel, 1987; Rampnoux et al., 1977) from the upper Pleistocene to Holocene show a differential uplift between the western side of Trois Fourches cap (Fig. 1 for location) which rises at a rate of 0.1 mm/year (Pedoja et al., 2013) and the eastern side (i.e. the Bou Areg sedimentary basin and the Nador lagoon) which subsides.

At the present-day, the Nador region is considered as the most active area of the northern Rif, together with the Al-Hoceima region. The moderate instrumental seismicity (IRIS catalog) is clustered along a roughly E-W-oriented, southward curved zone around Bou-Areg plain and Nador lagoon while the focal mecanisms, consistent with the geological observations, seem to indicate inverse faulting along the Kebdana massif associated to strike-slip faulting further north into the Bou Areg plain, and normal faulting offshore the Nador lagoon (Palano et al., 2013; Stich et al., 2007). Finally, the historical seismicity indicates that at least seven Mw > 5.5 earthquakes were recorded since the XVIth century in Melilla region (El Mrabet, 2005; Peláez et al., 2007).

3. Materials and methods

3.1. Seismic data acquisition

Twenty-four very high resolution (VHR) seismic profiles were acquired in the Nador lagoon, totalling about 57 km (Fig. 1C). The profiles were acquired in the northern part of the lagoon, where most cores have been collected. Four profiles intersect the position of three sediment cores. The seismic survey was performed using a boomer IKB-Seistec, characterized by a line-in-cone receiver that allows investigation of very shallow water settings (Simpkin, 1993). The central frequency of the Boomer IKB Seistec is about 5 kHz. During the survey, the trigger rate was 2 Hz, with power supply energy levels of up to 200 J. Data were recorded using the Delph-Seismic system and processed with Seismic Unix software. This consisted mainly of applying a frequency band pass band filter. A P-wave velocity of 1600 m/s was chosen for time-to-depth conversion, which is the value conventionally used for shallow, little compacted and rich in water sediments (Certain et al., 2004). Positioning was achieved by a DGPS, and simultaneously recorded by the Delph-Seismic system. Seismic data were then interpreted on the basis of seismic stratigraphic principles (Mitchum et al., 1977) for the identification of seismic facies and seismic units.

3.2. Core material

Prior to the seismic survey, five sediment cores, 0.48 to 1.78 m long, were collected in the lagoon using a UWITEC© gravity coring platform (University of Chambery and Laboratoire des Sciences du Climat et de l'Environnement). Four of them were located in the north-western area where the majority of the seismic data were collected. The location of the coring sites was determined using a handheld GPS providing a horizontal accuracy of 3 to 6 m (Fig. 1C). It is worth noting that all cores were refused on a hard layer which corresponds to silt interlaced with gypsum.

Each core was split lengthwise for sedimentary facies description and sampling for grain-size analyses using a Beckman Coulter © LS 13320. The sediment core was also analyzed by X-ray fluorescence (XRF) using an XRF core scanner with a step size of 0.5 mm in order to examine the major element geochemistry. AMS radiocarbon dating was carried out on intact shells. Measurements were conducted at the LMC14 Laboratory on the AMS ARTEMIS (CEA institute at Saclay, France). Absolute dating was corrected by applying a reservoir correction (R) of −218 years (Raji et al., 2015) and then calibrated using the calibration programme CALIB 7 (Stuiver and Reimer, 1993) and the Marine13 age calibration data from Reimer et al. (2013). Fifteen ^{14}C dates were used, including eight from the MC45 sediment core already published (Raji et al., 2015).

4. Results

4.1. Identification of major seismic units

Seven seismic units have been identified (from Us0 to Us6) on the VHR seismic data collected in the Nador lagoon. The unit Us0 is interpreted as the lagoon basement, whereas the units Us1 to Us6 compose the lagoonal sedimentary infill. The NW-SE seismic profile 09 images these seven units (Fig. 2). It should be noted that the seismic units Us1 to Us3 are only observed in the northern part of the lagoon. In the south, the deepest seismic unit that can be imaged is the Us4.

The seismic unit Us0 is the most basal unit. The base of this unit is not imaged due to the lack of penetration. Its upper boundary is an irregular surface, probably of erosional nature. Us0 is generally characterized by chaotic to transparent seismic facies and locally by some discontinuous and high to moderate amplitude reflectors (Fig. 3A).

The unit Us0 is observed mainly along the continental side of the lagoon and is assumed to represent its basement. This basement is represented by (i) the volcanic bedrock clearly visible close to Atalayoun, with a pronounced dip towards the lagoon (chaotic to transparent seismic facies) and (ii) the Plio-Pleistocene formations (discontinuous high to moderate amplitude reflectors) that overlie the volcanic unit.

The seismic unit Us1 fills the deepest topographic lows incised into the basement. It is only present to the north of Atalayoun. It does not exceed 3 m thick and is characterized by parallel, continuous and roughly horizontal, low to moderate amplitude reflectors (Fig. 3B). Its upper boundary is an erosional surface.

The seismic unit Us2 is composed of chaotic seismic facies or low to moderate amplitude reflectors with an oblique tangential configuration (Fig. 3C). Its lower boundary is an erosional surface, with local downlap terminations. The upper boundary is a surface with toplap terminations. On the barrier side of the NE-SW oriented seismic profiles, landward dipping reflectors are locally visible into Us2, attesting a landward progradation (Fig. 4).

The seismic unit Us3 is similar to Us1 in that it too fills the topographic low to the north of Atalayoun. It is mainly preserved on the landward side of the lagoon, and rests on the basement (Us0) and locally on Us2. Us3 contains chaotic seismic facies as well as discontinuous moderate amplitude reflectors with sigmoid clinoforms and channel like geometries (Fig. 3D). Its basal boundary is an erosional surface with local downlap terminations.

The seismic unit Us4 shows parallel and roughly horizontal continuous high amplitude reflectors (Fig. 3E). Its upper boundary is an erosional surface with toplap terminations. North of Atalayoun, Us4 rests on Us3 along an erosional surface. In the south, Us4 is the lowest seismic unit to be imaged as the acoustic signal does not penetrate deeper (Fig. 3F and Fig. 5).

The seismic unit Us5 is mainly observed on the lido side of the lagoon. Generally, it has a chaotic facies, but shows locally low to high

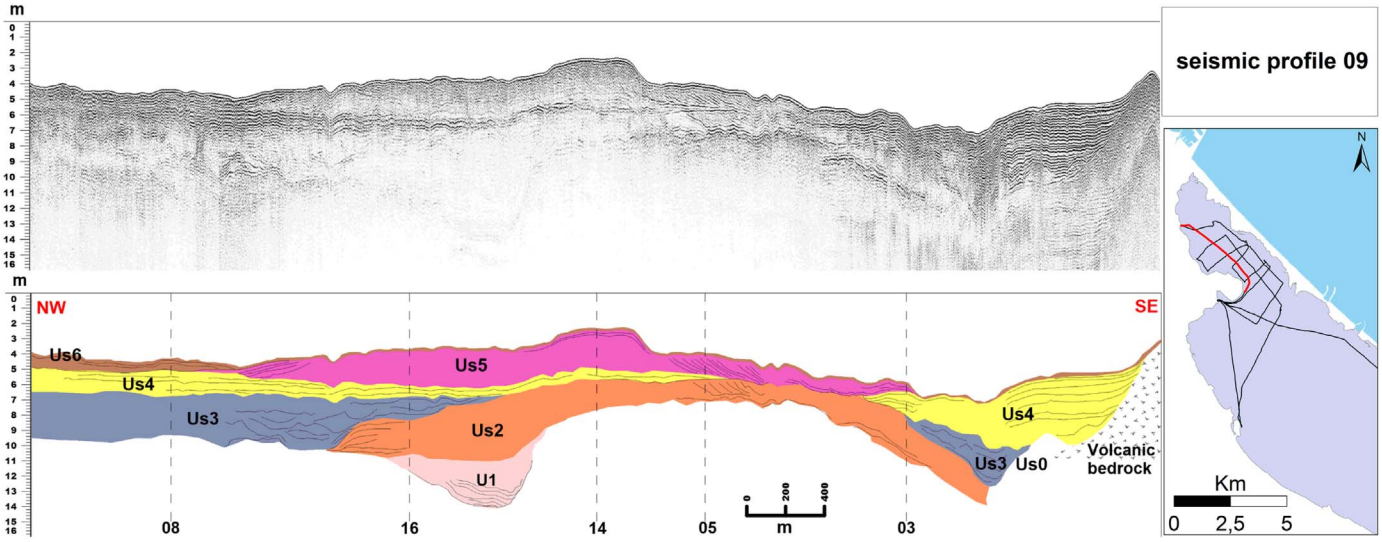

Fig. 2. Seismic profile 09 imaging the six seismic units (from Us1 to Us6) that comprise the Nador lagoon infill above the geological basement (Us0). The dotted lines indicate intersection with other seismic profiles.

amplitude moderately-continuous and gently dipping reflectors (Fig. 3G). Locally, sigmoidal and tangential reflectors are present. Like Us2, the directions of dip are mainly landward as well as NE-SW (i.e. shore parallel). These directions allude to a general lobe geometry with a landward progradational arrangement (Fig. 4).

The seismic unit Us6 is the uppermost unit. Its thickness does not exceed 1 m. Us6 shows parallel and subhorizontal reflectors of high amplitude and good continuity. Us6 forms a drape and rests conformably on the underlying units. Its upper surface corresponds to the lagoon floor.

4.2. Geochemical characterization, lithostratigraphic units and chronology

4.2.1. Surface sediment

Based on the significance of their concentrations and uncertainties detected by mobile analyzer, eight elements have been selected for the surface sediments (Al, Fe, K, Ti, Rb, Ca, Si and Sr). The Principal Component Analysis (PCA) was adopted to define the proximities between the geochemical elements and to identify different groups of common origin and process (Fig. 6a). The factor 1 expresses 67.97% of the variance and allowed the identification of two groups: the first group is composed of Fe, Ti, K, Rb and Zr (positive loadings) which characterizes the terrigenous samples and the second group composed of the Ca, Si (positive loadings) is mainly of marine origin. The spatial distribution of the concentrations of Fe, Ti, in the surface sediments shows that maximum levels are found mainly on the continental part of the lagoon (Fig. 7). In contrast, high concentrations of Ca and Si are found towards the sea. On this basis, the inter-element ratios such as Si/Al, Ca/Fe or Sr/Fe can be used to trace marine sediment inputs in the Nador lagoon.

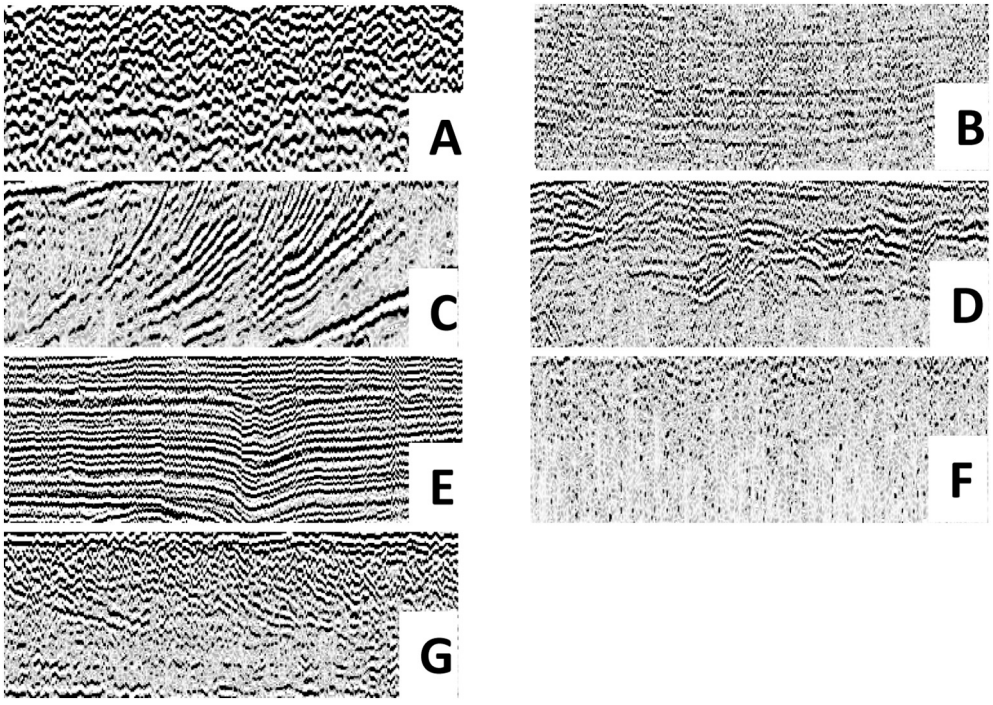

Fig. 3. The main seismic facies distinguished on the very high resolution seismic profiles acquired in the Nador lagoon (see text for explanation).

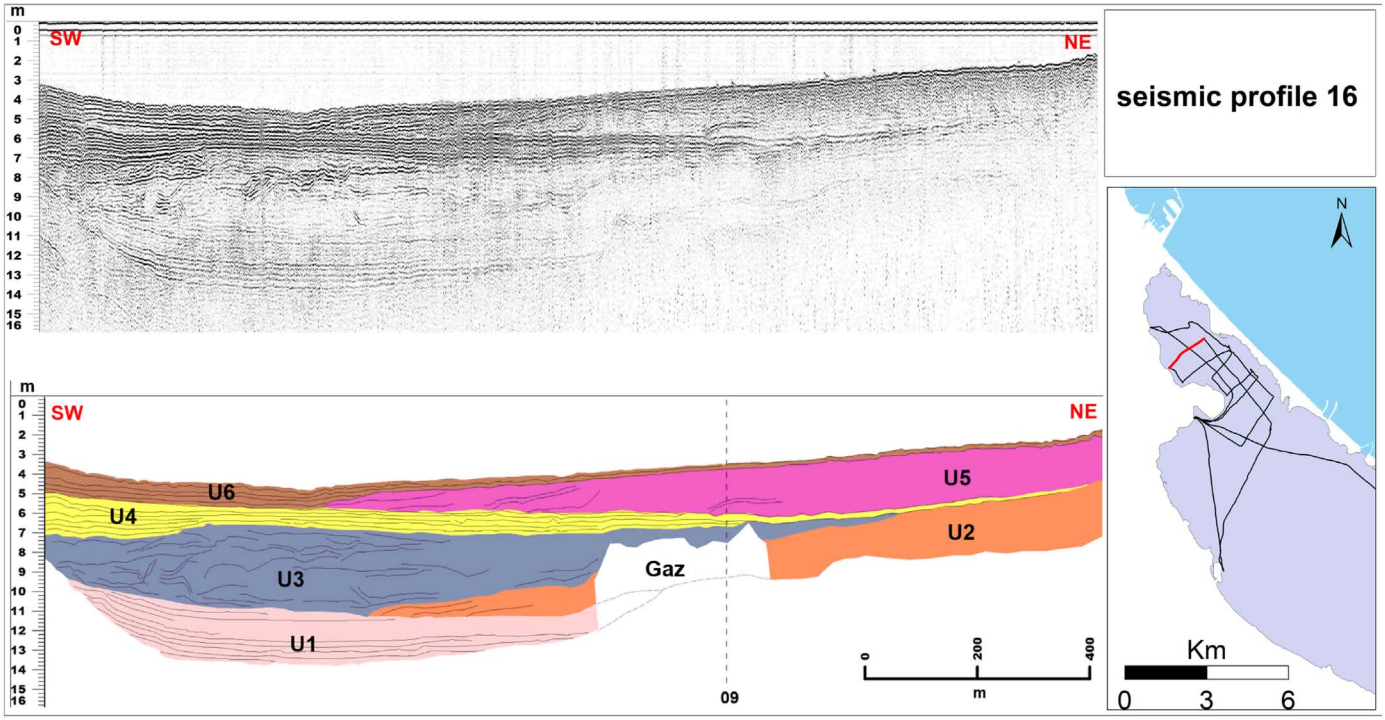

Fig. 4. Seismic profile 16. This line shows arrangement of seismic units according to a NE-SW profile orientation. The general lobe geometry of the seismic unit Us5 with a landward progradation is clearly observed on this profile.

4.2.2. Sediment cores

In the sediment cores, the PCA shows that about 68.15% of the total variation is explained by the first principal component (Fig. 6b). Two groups are identified, a group composed of Al, Fe, Ti, K, Rb exhibits similar variations and shows enrichment peaks in fine-grained sediments. In contrast, Sr, Ca and Si enrich the coarse sediments, except for the bottom of sediment cores where exceptional values are observed in Sr and Ca and are associated with evaporitic sediments.

Fig. 8 shows the spatial correlation between the multi-proxy analysis of the sediment cores, the percentage of 133–282 µm sand population is used as an indicator of marine sands (Raji et al., 2015) and the fine grained sediments (< 63 µm) trace sediments from the watershed. Similarly, the Si/Al ratio is selected to differentiate marine inputs from those inputs coming from the watershed.

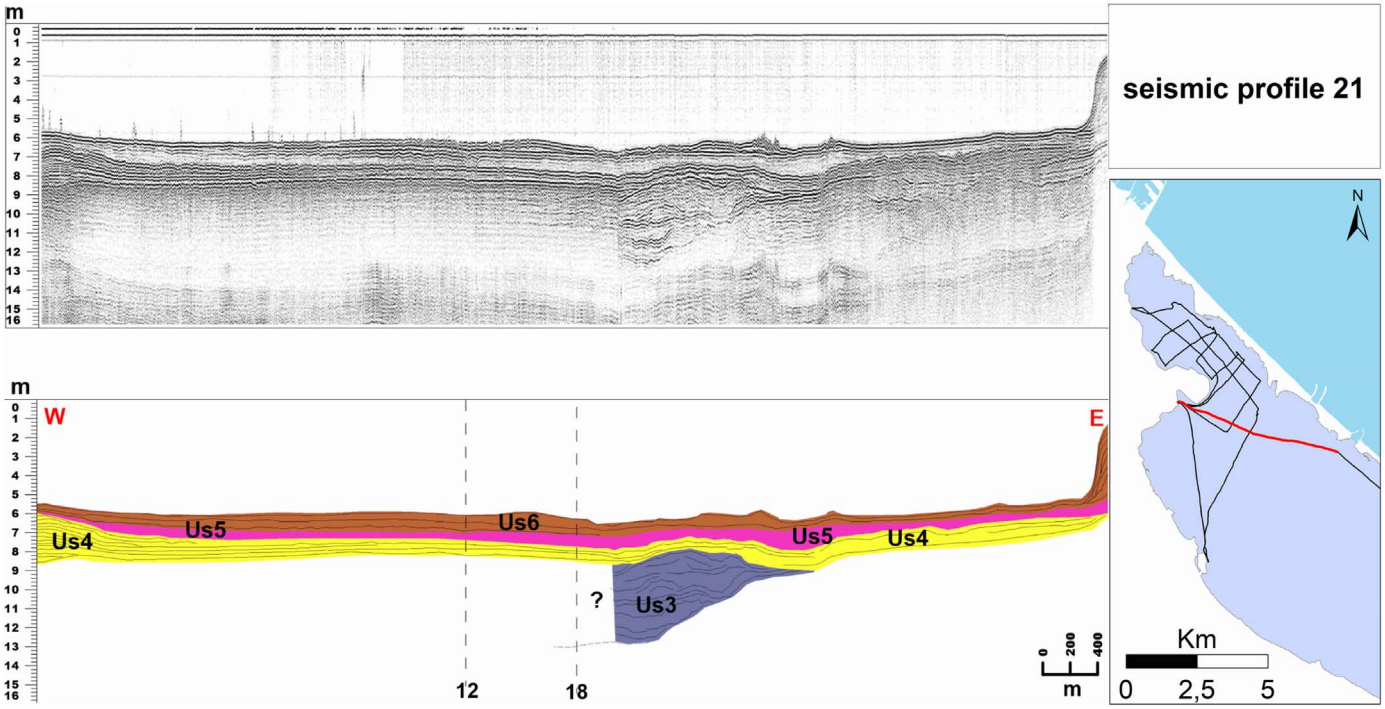

Fig. 5. Seismic profile 21. On this line, acquired in the northern part of the southern basin of the lagoon, only three seismic units, Us4 to Us6 are imaged throughout. Local occurrences of Us3, are evident. The acoustic turbidity observed laterally to Us3 is interpreted as a lack of penetration of the acoustic signal due to the presence of a gypsum layer rather that of gas.

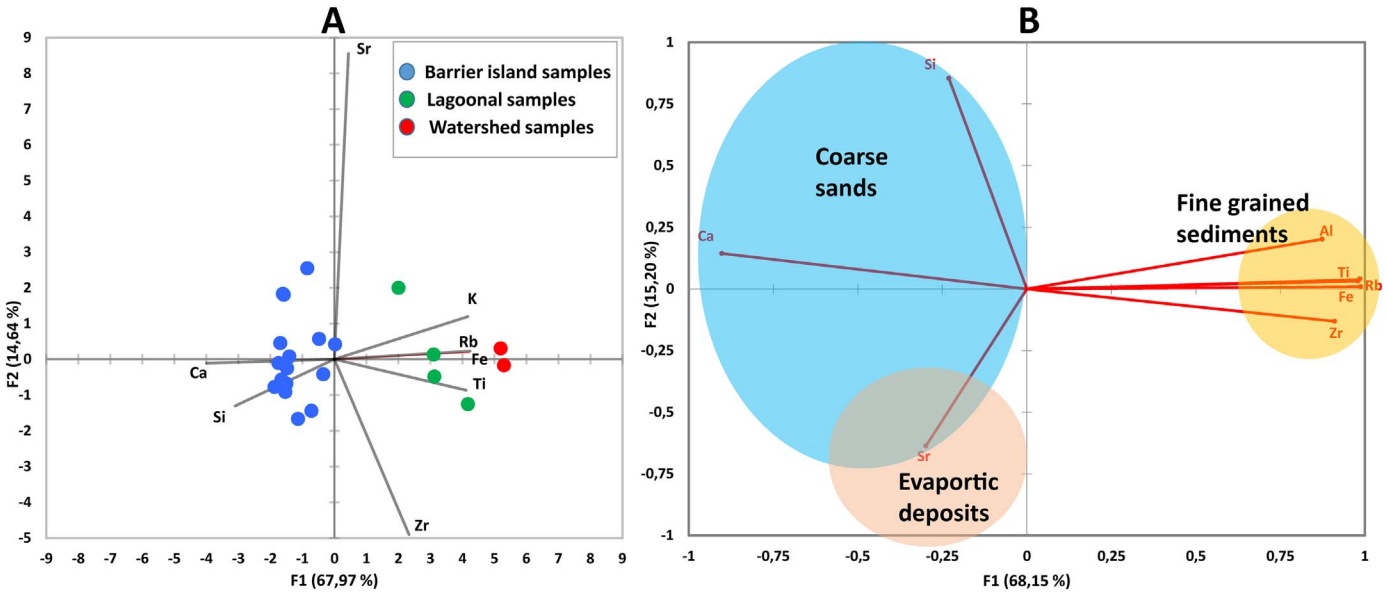

Fig. 6. Principal component analysis of Nador geochemical data from: (A) the surface sediments and (B) the core sediments.

Based on these various analyses, including radiocarbon dating (Table 1), four distinct lithostratigraphic units have been recognized from base to top (Fig. 8):

- Unit 1 is composed of silty laminae and silty sand laminae associated with gypsum crystals. It is present at the base of cores MC44, MC45, MC33. Maximum concentrations of Sr is found in this unit. According to the AMS dating, this basal unit is older than 1200–1000 CE.
- Unit 2 consists mainly of homogeneous, fine-grained brown silt locally rich in shell fragments. Thin parallel laminations mark the top of the unit. In core MC33, the unit 2 is composed of coarse grained silty sand and it is absent in MC34 and MC22. Geochemically this unit is rich in terrigenous elements but also shows a slight increase in Ca and Sr and lower Si/Al ratios. Dates indicate that the age of Unit 2 ranges from about 1200 to 1500 CE.
- Unit 3 is dominated by coarse sand in MC44, MC34 and MC33, with a maximum percentage of the 133–282 μm grain size population and with peaks of Si/Al. In MC45 fine grained red silty to sandy silt layers are intercalated with the coarse sand (that shows peaks of Si/

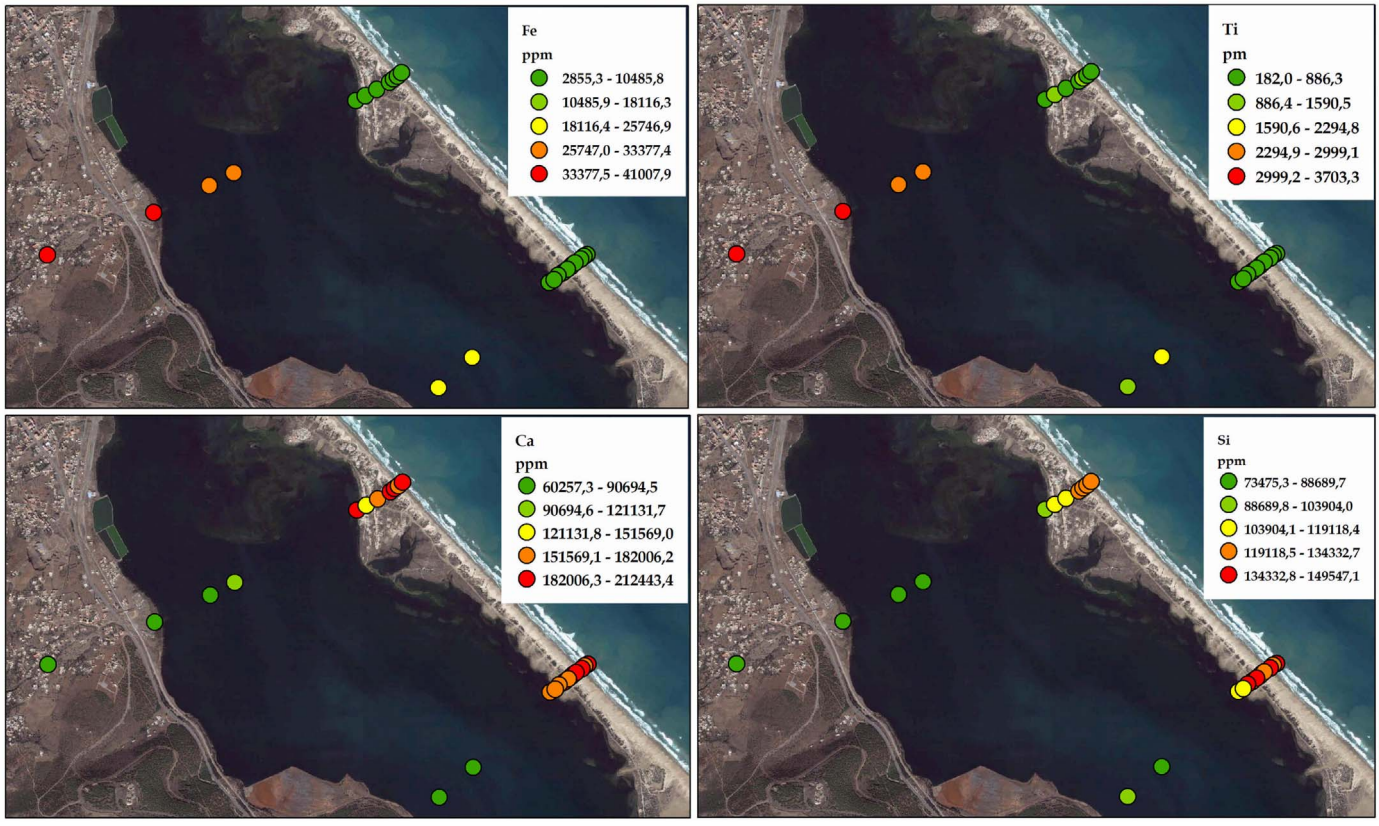

Fig. 7. Maps of iron, titanium, calcium and silicon contents values along sea–lagoon–continental orientated transects.

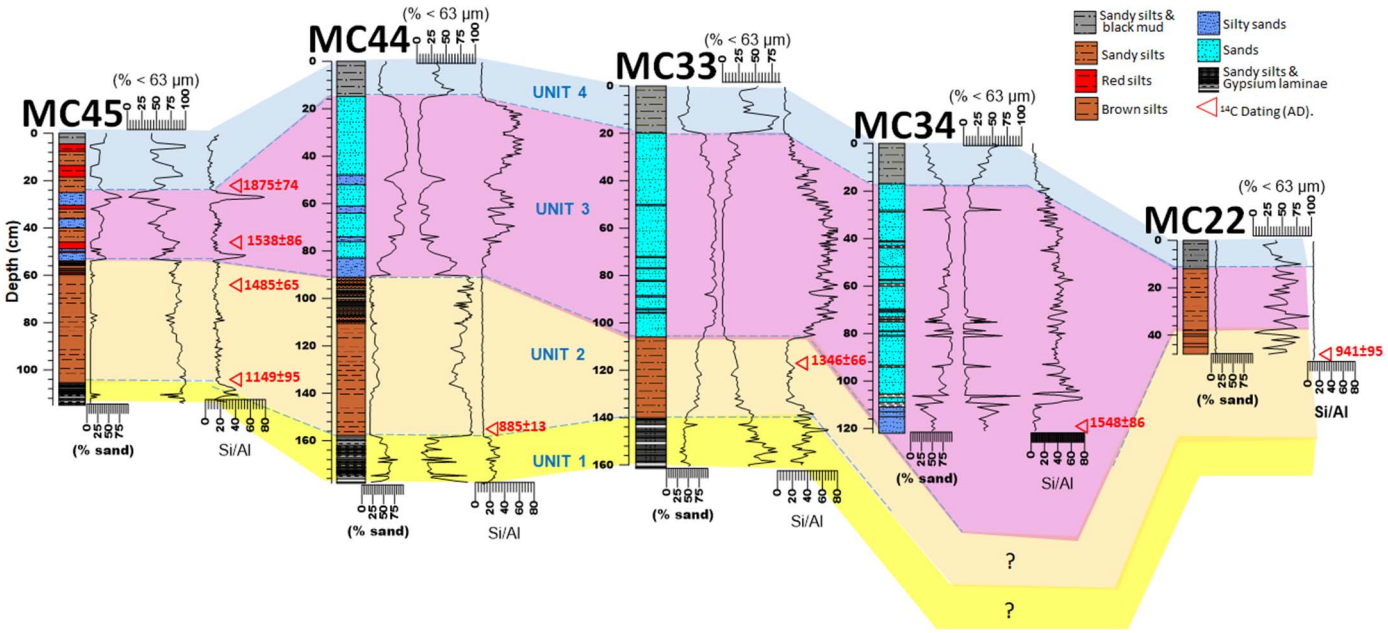

Fig. 8. Sediment cores collected in the Nador lagoon (cf. Fig. 1C for location). Three main sedimentary units are recognized and dated (AMS radiocarbon ages calibrated CE). A correlation across the lagoon between the units is proposed according to sedimentary facies, Si/Al geochemical ratio content, < 63 µm fine-grained sediments percentage and 133–282 µm sand percentage.

Table 1
Radiocarbon ages obtained on mollusk shells collected along sediment cores retrieved from the Nador lagoon. ^{14}C ages are calibrated using the Marine13 calibration curve with reservoir age ΔR of −218, model ages were obtained by Clam code-package.

Code lab	Core	Materiel	Depth (cm)	$d^{13}C$	Age ^{14}C (BP)	Age cal. (CE)
SacA 28609[a]	MC45	*Loripes lacteus*	22	4,8	235 ± 30	1875 ± 74
SacA 26943[a]		*Cerastoderma glaucum*	32	2,4	730 ± 30	1392 ± 65[b]
SacA 26944[a]		*Cerastoderma glaucum*	46	0,7	575 ± 30	1538 ± 86
SacA 26945[a]		*Cerastoderma glaucum*	50	2,4	630 ± 30	1476 ± 59[b]
SacA 28610[a]		*Cerastoderma glaucum*	56	3,8	645 ± 30	1468 ± 58[b]
SacA 28611[a]		*Parvicardium exiguum*	64	4	620 ± 30	1485 ± 65
SacA 26946[a]		*Acanthocardia mucronata*	91	4,4	1340 ± 30	834 ± 107[b]
SacA 26947[a]		*Cerastoderma glaucum*	104	6,5	1035 ± 30	1149 ± 95
SacA 31692	MC44	*Cerastoderma glaucum*	155	5,6	1295 ± 30	885 ± 103
SacA 28612	MC34	*Cerastoderma glaucum*	17	4,7	545 ± 30	1557 ± 85[b]
SacA 28613		*Cerastoderma glaucum*	76	2,7	770 ± 30	1373 ± 64[b]
SacA 28614		*Acanthocardia mucronata*	106	7,9	580 ± 30	1534 ± 85[b]
SacA 28615		*Acanthocardia mucronata*	119	4,8	560 ± 30	1548 ± 86
SacA 31690	MC33	*Cerastoderma glaucum*	117	0,4	825 ± 30	1346 ± 66
SacA 28609	MC22	*Cerastoderma glaucum*	48	5,1	1235 ± 30	941 ± 95

[a] Raji et al. (2015).
[b] Inversed age.

Al ratio) and marine sand. In MC22, the Unit 3 occurs as a silt dominated interval. The age of Unit 3 extends from about 1500 to 1800–1900 CE.

- Unit 4 consists of a dark fine grained sandy silt and lagoonal mud, enriched in organic matter and shell fragments. This unit is rich in terrigenous elements and is characterized by high concentrations of Br and Pb. Ages demonstrate that Unit 4 records the last century of deposition into the lagoon.

4.3. Correlation between core and seismic data

The cores collected in the Nador lagoon (including those examined in the studies by Irzi, 2002; Mahjoubi, 2001, do not intersect all the seismic units. However, it is worth noting that the penetration of all cores was stopped by a hard layer which corresponds to the upper part of the seismic unit Us4. Hence, the sediment cores allow ground-truthing of only three seismic units (Us6, Us5 and the upper part of Us4) (Fig. 9):

- The upper part of Us4 corresponds to the sedimentary unit 1 (evaporitic sediments, older than 1200 CE) and to the sedimentary unit 2 (silt dominated deposits, dated between 1200 and 1450 CE).
- The seismic unit Us5 corresponds to the sedimentary unit 3 (mostly dominated by marine sands on the seaward side of the lagoon, evolving gradually to fine-grained silt on the watershed side. In all cores, the deposition of this unit begins at around 1450 CE).
- The seismic unit Us6 corresponds to the sedimentary unit 4 (recent lagoonal fine grained mud).

As in the example described by Billeaud et al. (2005), a good correlation between the main reflectors and the limits of sedimentary units corresponding to major grain size change was observed.

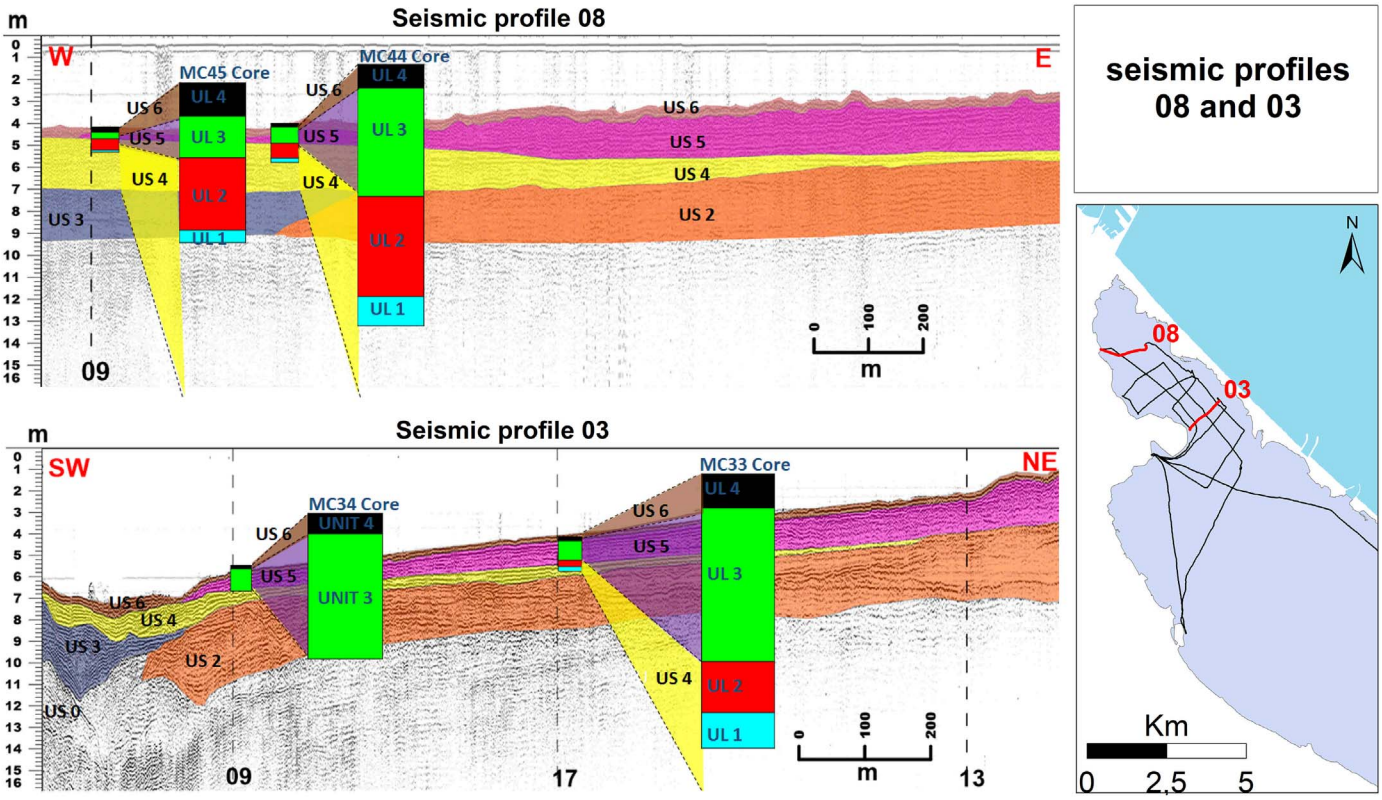

Fig. 9. Correlation between sedimentary/lithostratigraphic units and seismic units on seismic profiles 08 and 03 acquired in the northern basin of the Nador lagoon.

5. Discussion

5.1. Lagoon sedimentary infill stages

In the northern part of the lagoon a minimum of 4 m and a maximum of 9 m of layered sediment covers the bottom of the Nador lagoon. For the rest of the lagoon, the lack of seismic imaging below Us4 prevents the specifying of the thickness of the sedimentary fill. In the northern basin of the lagoon, the seismic data allow a pseudo 3D reconstruction of the geometry and arrangement of the seismic units to be identified (Fig. 10). This reconstructed architecture, complemented with the core and chronological data, show that the sedimentary infilling of the Nador lagoon comprises at least three main stages:

The *first Stage* corresponds to the infilling of a paleo-valley to the north of Atalayoun by the seismic units Us1 and subsequently by Us2, with landward dipping reflectors, and Us3, with seaward dipping reflectors. This stage attests for significant sediment inputs from both marine and fluvial sources.

The *second Stage* is marked by the deposition of seismic unit Us4 which is pervasive throughout the lagoon. Sediment cores demonstrate that the upper part of Us4 corresponds to an evaporitic episode that occurred before 1200 CE. A fine-grained sedimentation phase followed this episode, lasting from 1200 to 1500 CE. In similar environments around the world, the gypsum crystals associated with clay layers are

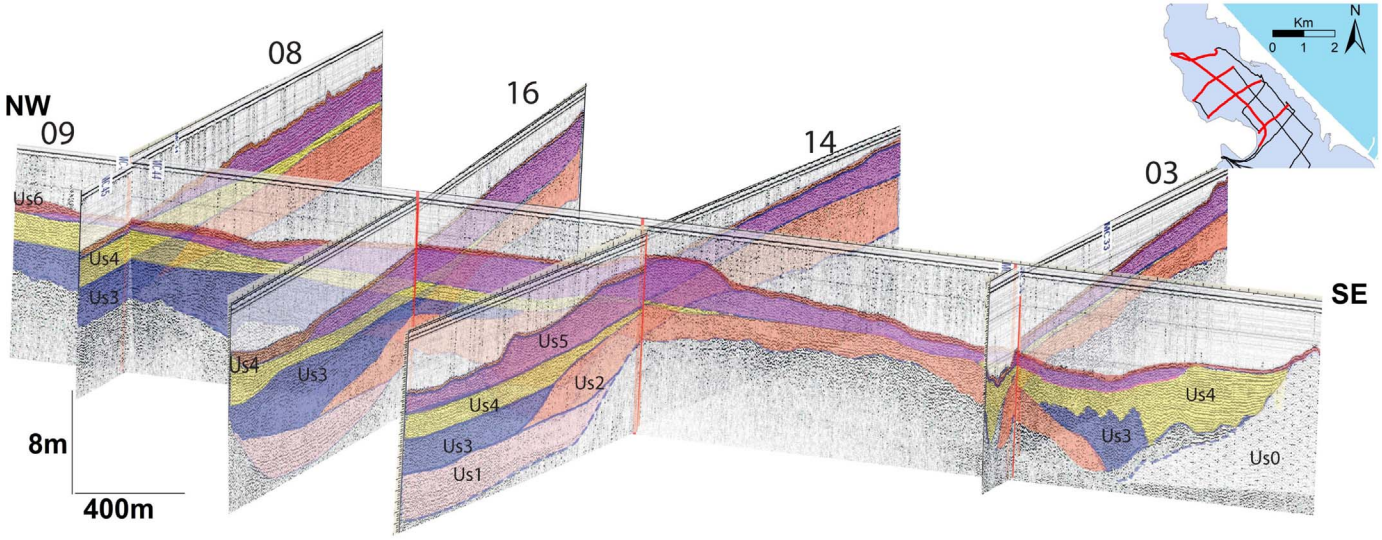

Fig. 10. Pseudo-3D fence diagram reconstruction of the sedimentary infill of the northern basin of the Nador lagoon based on seismic data.

generally described as formed following closure of the lagoon by barrier island sealing and decline in the fresh water delivery (Arakel, 1980; Khawfany et al., 2017; Levy, 1974). During this second stage of infilling, we thus assume that the Nador lagoon was partially to completely isolated from the sea favoring salt marshes (*Sebkha*) development. The quiet-water conditions of the sheltered lagoon led to fine-grained sedimentation and, during severe droughts, to evaporite formation. This scenario is also supported by the fact that the sedimentary unit 1 is deposited as part of the Medieval Climate Anomaly (MCA ~ 1150–650 cal year BP). This latter is known in the western Mediterranean by predominant arid conditions and a decrease in the fluvial inputs (Nieto-Moreno et al., 2011).

In contrast to the second stage, the *third Stage* appears to be very dynamic. It extends from 1500 CE to the present and is marked by the deposition, from the 15th to 19th centuries, of the seismic unit Us5 which is mainly composed by coarse sands originating from marine sources. Compared to Stage 2, marine incursions into the lagoon drastically increased during this third stage of infilling. After the 19th century, the marine influence was still significant but generally weaker as testified by the widespread deposition of fine-grained sediments (Us6).

5.2. The Nador lagoon between the 15th and 19th century: what happened?

In the Nador lagoon, the 15th -19th century sand body covers most of the NW area of the lagoon and displays landward progradational features over a distance of 1.5 to 4 km, with thicknesses up to 150 cm close to the landward side (Fig. 10). The upper part of the MC45 sediment core, collected only 500 m from the landward shore and about 1.5 km from the barrier (Fig. 1), shows an interval with several marine sand layers intercalated within watershed/terrestrial and lagoonal sediments, suggestive of multiple marine sand entrainment and deposition events (Raji et al., 2015). In addition, the progradational reflectors contained in the seismic unit Us5 confirm that this unit developed landward by successive steps between about 15th -19th century (Fig. 4).

The 15th to 19th century period appears as a critical episode of the Nador lagoon evolution marked by thick marine sand lobes extending far landward (Seismic Unit Us5/sedimentary Unit U3). In coastal lagoons, fan-shaped sedimentary bodies extending from the sandy barrier into the back-barrier are generally interpreted as the result of extreme sea levels induced by storms or tsunamis (Luque et al., 2001; Matias et al., 2008). These bodies occur where storm or tsunami waves cut through and overtop the barrier, washing lobes of sandy beach sediment into the back-barrier lagoon (Scour fans and washover fans e.g., Donnelly et al., 2004; May et al., 2012). Nevertheless, lagoonal sand barrier topography is frequently subject to changes by coastal erosion. These changes can deeply affect their sensitivity to marine events (Tsunamis/storms). A decrease in dune barrier elevation for example allow smaller marine surges to penetrate inland and deposit sandy sediments into back barrier environments (Benallack et al., 2016; Dezileau et al., 2011; Gomes et al., 2017). For the Nador lagoon's sandy barrier, historical topographic information is limited. At present, it has a height of 1–3 m which appears to have been constant for at least the past 100 years (Carpio, 1995; Raji et al., 2013). For a longer period, we cannot assume that the barrier has remained at the same height. It therefore seems appropriate to consider that the Nador lagoon barrier may have been sufficiently low and narrow to have allowed full inundation. However, recognizing this does not prevent us from admitting that a positive relationship exists between event intensity and the size of the overwash sand body (Dezileau et al., 2011). Furthermore, Donnelly et al. (2004) demonstrate that only the major storms leave a stratigraphically distinct and regionally consistent record of overwash sand layers in the sediments of the coastal marshes. In addition, the lagoonal, shell-rich clay/silt sediments appear throughout the MC33, MC45 and MC44 sediment cores before the 15th century, and indicate that the study site was likely protected behind the barrier system over that time.

On the other hand, the base of the 15th century sandy unit is an erosional base that indicates a sudden and energetic marine dynamics. Furthermore, the presence in the MC45 sedimentary core of a succession of 3 sandy layers separated by lagoon shell-rich clay/silt sediments shows that the area was alternatively under the influence of marine storms and of quiescent conditions between the 15th century and 19th. All these arguments allow us to favor the hypothesis of catastrophic events that were to deposit the marine sands over large distances in the back barrier lagoon. Indeed, owing to its geographical location, the Nador area is cited as a vulnerable area to extreme marine floods caused by storm surges and tsunamis. Although in some case studies, the distinction between storm and tsunami deposits was possible (Goff et al., 2004; Nanayama et al., 2000), it remains a matter of controversy (Engel et al., 2010; Morton et al., 2007). Storm deposits share many characteristics with tsunami deposits and even until today the sedimentological proxies are not sufficient to differentiate between the two (Judd et al., 2017; Puga-Bernabéu and Aguirre, 2017). Multi-proxies studies using palaeontological, geochemical and geomorphological characteristics are necessary to provide relatively strong evidence to discriminate them (Costa et al., 2017; Judd et al., 2017). In the following sections, we discuss the probable genetic mechanisms of the marine sand unit preserved in the Nador lagoon, in the light of our knowledge of the regional context. These include storm surges (Raji et al., 2013), tsunamis (Gonzalez et al., 2010) and other earthquake-related processes.

5.2.1. Tsunami events in the Nador area

No evidence of uprush and backwash successions was observed in our sediment cores. However, the large extension of the sand bodies such as that documented for the Nador lagoon generally reflect a tsunami origin according to a number of studies (e.g. May et al., 2012; Morton et al., 2007). To examine this possibility, we have listed the historical events that occurred since 1500 CE which might have had an impact on the Moroccan coast. Four tsunamis are reported (Kaabouben et al., 2009), in 1522, 1680, 1790 and 1856. However, apart from the descriptions of these events, except for the 1522 tsunami, the impacts in the Nador area were minor and cannot explain the large inundations of our record. On the other hand, two facts may suggest that the 1522 tsunami could have impacted the study area: (i) a 1522 tsunami deposit was found in Cabo de Gata lagoon (Almeria, Spain) 190 km North of Nador (Reicherter and Becker-Heidmann, 2009); (ii) the village of Badis-Ghomera, located on the Mediterranean coast of Morocco, about 100 km West of Nador, was probably impacted by the 1522 tsunami waves (Kaabouben et al., 2009). Hence, the Nador lagoon, being located < 180 km south of Almeria where the maximum intensity of the tsunami occurred, should have been directly exposed to the 1522 event.

The above arguments are however unlikely to justify a definite impact on the Nador lagoon by the 1522 tsunami, still less to explain the large extension of marine sands. Indeed, this tsunami event is not reported in local chronicles of Melilla, located 2 km NW of the lagoon. Nonetheless, Louis de Marmol, a Spanish historian and traveller of the 16th century, reported in 1573 (in Carpio, 1995) that 18 years prior to his account (i.e.1555) an inlet opened naturally through the Nador lagoon barrier. Additionally, the oldest historical map of the study area, produced in 1576 (Fig. 11), shows that the barrier was very thin, particularly in the NW, barely separating the lagoon from the Mediterranean Sea.

5.2.2. Mediterranean storms

Storms deposits are generally considered to have smaller spatial dimensions when compared to tsunami deposits, their deposition being typically restricted to a zone of a few hundred meters from the shore (Judd et al., 2017; May et al., 2012; Morton et al., 2007). However, exceptionally large storms such as tropical events are capable of moving

Fig. 11. The present-day morphology of the Nador lagoon barrier (2014, Google Earth image) compared with that of the second half of the XVIth century (historical map of 1576, Álvarez Terán, 1980).

sediments over long distances (Zong and Tooley, 1999). The most powerful Mediterranean storms (tropical-like storms) are uncommon in the Nador region (Tous and Romero, 2011) but their past existence cannot be excluded. Indeed, evidence for old inlets and large washovers attributed to extreme storms of the last century are observable in the Nador lagoon barrier island (Hamoumi, 2012; Raji et al., 2013). Moreover, Raji et al. (2015) identified one of the sand layers sampled in the MC45 sediment core (situated at over 1.2 km from the lido) as the landward extent of a backbarrier washover created in the wake of an 1889 storm event which was caused by north-to-northeast winds resulted in a 150 m wide inlet to form. It is therefore clear that in the case of the Nador lagoon, extreme storms were able to transport marine sand over large distances especially after breaching events. Importantly, it is worth noting that the time interval of the sand body, i.e. 16th–19th centuries, is coincident with the Little Ice Age (LIA), a period that is characterized by higher frequency and intensity of storms in the western Mediterranean (e.g. Camuffo et al., 2000; Degeai et al., 2015; Dezileau et al., 2011; Sabatier et al., 2012; Shah-hosseini et al., 2011). Accordingly, we might expect the breaching of the barrier under storm wave action associated with the LIA climatic conditions, resulting in several short barriers separated by large inlets (Fig. 12). This partial destruction of the lido would have led to a greater transportation of marine sands into the lagoon. We thus believe that the sand body deposited between the 15th and 19th centuries in the Nador lagoon can result from the enhanced storm wave activity of the LIA. This hypothesis is also favoured by the presence in the sedimentary cores (MC4, MC33 and MC34; Fig. 8) of a succession of sandy layers (enriched in marine elements such as Ca, Sr etc.) intercalated by thin fine-grained layers of terrestrial elemental enrichment.

5.2.3. Co-seismic subsidence and sand liquefaction

The Nador lagoon is located in a subsiding area and belongs to one of the most seismically active regions of the Mediterranean. This compels us to consider two earthquake-related impacts on the Nador lagoon, independent of tsunami generation (i) co-seismic subsidence and ii) sand liquefaction.

Co-seismic subsidence is known in similar environments such as along the Pacific Northwest coast of the USA (Kelsey et al., 1998; Witter et al., 2001; Nelson et al., 2006; Leeper et al., 2017) or along the West Coast of New Zealand (Nichol et al., 2007). Co-seismic subsidence causes an increase in local relative sea level that facilitates extreme wave runup reaching areas that would not have been flooded under normal conditions and induces marine flooding of back barrier environments. Witter et al. (2001) considered inter or post-seismic sea-level change as a temporary situation and stated that a period of 50 to 170 years is necessary to restore the sea level prior to the earthquake in their study area.

Earthquakes can also affect coastal lagoons due to liquefaction processes. Indeed, the seismic shock can liquefy the sands of the barriers, favoring erosion and triggering the formation of breaches connecting the lagoons to the sea (Greene et al., 1991; Minoura and Nakaya, 1991).

In historical archives, earthquake effects on the Nador lagoon area are rarely mentioned. For example, strong seismic activity is described between 1887 and 1888 but no further details were elaborated on (in Nieto, 1996). It is worth noting that the closure of inlets of the Nador lagoon is reported as a series of coastal changes associated with the 1755 and 1848 earthquakes (Carpio, 1995), suggesting that sand liquefaction could have concomitantly affected the barrier during these events. Nonetheless there is no evidence that earthquakes could have induced breaching processes.

We thus propose that relative sea-level rise, as well as sand liquefaction related to high, localized seismic activity, should be considered as factors in the destabilization of the Nador lagoon barrier. These could

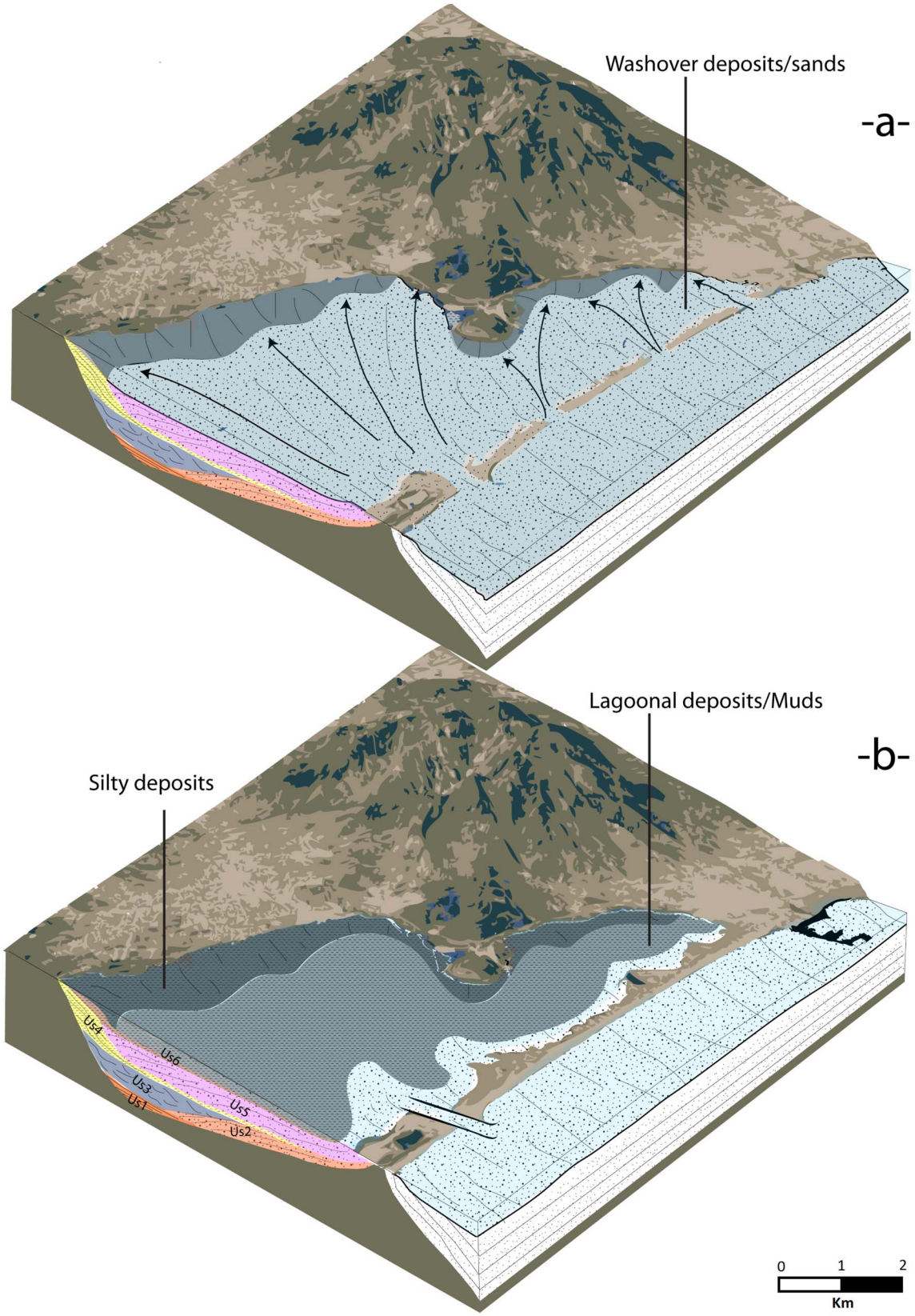

Fig. 12. Diagram showing the abnormal expansion of marine sands (a) compared to the current situation of the NW part of the Nador Lagoon (b). A narrow barrier, breached under the action of storm waves into several short barriers separated by inlets can explain the large distance of marine sediment transportation (a).

partly account for the deposition of marine sands into the lagoon, especially between the 15 and 19th centuries marked by enhanced storm dynamics (LIA).

Finally, it is worth noting that the deposition of seismic unit Us2, according to its stratigraphic position, occurred prior to 1000 CE. Us2 displays a comparable internal architecture to that of Us5 with

landward progradational reflectors. This analogy suggests that Us2 can be interpreted as a washover fan similarly to Us5. We thus expect that Us2 could be also related to a period of enhanced marine storm dynamics that occurred before the LIA, i.e. between 1950 and 1400 BP, the impact of which has been recorded in French Mediterranean lagoons (Dezileau et al., 2011; Sabatier et al., 2012).

6. Conclusions

The objective of the present work was to study the history of the sedimentary infilling of the Nador lagoon by integrating for the first time core and seismic data. The cores provided sedimentological and age information of the last millennium of the infill, whereas very high-resolution seismic data allowed the imaging of the whole infill and the recognition of six distinct units of deposition. On the basis of the integrated core and seismic data set, two main stages of marine sand infilling separated by a period dominated by fine-grained sedimentation were identified. The youngest sand unit occurred between 1500 and 1900 CE, i.e. during the Little Ice Age. Enhanced storm activity of the LIA is believed to explain this stage of sand-dominated deposition into the lagoon. These results are consistent with similar studies in France and Spain and provide a better understanding of the impact of climate variability on extreme events on the Mediterranean basin. However, historical archives demonstrate that the tectonic context of the Nador area, resulting in earthquakes and probably tsunamis, should be considered together with the climatic conditions to fully understand the evolution of this western Mediterranean lagoonal environment. The Nador lagoon has been historically exposed to dynamic events that pose risks for infrastructure situated proximal to the coastline. We conclude that the coastal barrier is not suitable for urban development. Coastal risk management planners, therefore, need to consider this information for the growing urbanization linked to the tourism industry in the area.

Acknowledgments

The authors would like to thank all participants in the coring expedition particularly E. Regnier (Technician, LSCE – IPSL, Paris) and Pr. P. Blanchemanche for their collaboration in the various stages of this study. The authors wish to thank also the staff of MarChica Med Company (Rabat and Nador) for their assistance during the period of the coring expedition and in the preparation and execution of the seismic surveys. We thank the Laboratoire de Mesure ^{14}C (LMC14) ARTEMIS at the CEA Institute at Saclay (French Atomic Energy Commission) for the ^{14}C analyses. This study was funded by the MISTRALS/PALEOMEX project (Coord. Sicre, M.A., Guyot, J., Dezileau, L.) and PHC Volubilis (MA/11/253; coord.: L.Dezileau & M. Snoussi).

References

Ait-Brahim, L., Chotin, P., Tadili, B.A., Ramdani, M., 1990. Failles actives dans le Rif central et oriental (Maroc). Comptes Rendus Académie Sci. Sér. 2. Mécanique Phys. Chim. Sci. Univers Sci. Terre 310, 1123–1129.

Álvarez, T., 1980. Concepción Mapas, Planos y Dibujos. Archivo General de Simancas Vol. I Valladolid, Catálogo XXIX.

Arakel, A.V., 1980. Genesis and Diagenesis of Holocene Evaporitic Sediments in Hutt and Leeman Lagoons, Western Australia. J. Sediment. Res. 50, 1305–1326.

Barnes, R.S.K., 1980. In: CUP Archive (Ed.), Coastal Lagoons: The Natural History of a Neglected Habitat. XI Cambridge University Press (106 pp.).

Barusseau, J.P., Akouango, É., Bâ, M., Descamps, C., Golf, A., 1996. Evidence for short term retreat of the barrier shorelines. Quat. Sci. Rev. 15, 763–771.

Benallack, K., Green, A.N., Humphries, M.S., Cooper, J.A.G., Dladla, N.N., Finch, J.M., 2016. The stratigraphic evolution of a large back-barrier lagoon system with a non-migrating barrier. Mar. Geol. 379, 64–77.

Billeaud, I., Chaumillon, E., Weber, O., 2005. Evidence of a major environmental change recorded in a macrotidal bay (Marennes-Oléron Bay, France) by correlation between VHR seismic profiles and cores. Geo-Mar. Lett. 25, 1–10.

Bloundi, M.K., 2005. Etude Géochimique de la Lagune de Nador (Maroc Oriental): Impacts Des Facteurs Anthropiques (Thèse de Doctorat). Univ. Mohammed V, Fac.Sci. Rabat & ULPEOST, Strasbourg 1 (238 pp.).

Camuffo, D., Secco, C., Brimblecombe, P., Martin-Vide, J., 2000. Sea storms in the Adriatic Sea and the Western Mediterranean during the last millennium. Clim. Chang. 46, 209–223.

Cañedo-Argüelles, M., Rieradevall, M., Farrés-Corell, R., Newton, A., 2012. Annual characterisation of four Mediterranean coastal lagoons subjected to intense human activity. Estuar. Coast. Shelf Sci., Research and Management for the Conservation of Coastal Lagoon Ecosystems 114, 59–69.

Carpio, M.J.L., 1995. Mar Chica o sebja de bu-Areg: estudio geomorfológico y paleoambiental de la laguna de Melilla. Universidad de Murcia, Colección de Geografía. ed (173 pp.).

Carvalho do Amaral, P.G., Fonseca Giannini, P.C., Sylvestre, F., Ruiz Pessenda, L.C., 2012. Paleoenvironmental reconstruction of a Late Quaternary lagoon system in southern Brazil (Jaguaruna region, Santa Catarina state) based on multi-proxy analysis. J. Quat. Sci. 27, 181–191.

Certain, R., Tessier, B., Courp, T., Barusseauet, J.-P., Pauc, H., 2004. Very high resolution seismic investigation of the sedimentary infill of the Leucate lagoon (Aude and Pyrénées-Orientales – SE France). Bull. Société Géologique Fr. 175, 35–48.

Chaumillon, E., Bertin, X., Fortunato, A.B., Bajo, M., Schneider, J.-L., Dezileau, L., Walsh, J.P., Michelot, A., Chauveau, E., Créach, A., Hénaff, A., Sauzeau, T., Waeles, B., Gervais, B., Jan, G., Baumann, J., Breilh, J.-F., Pedreros, R., 2017. Storm-induced marine flooding: lessons from a multidisciplinary approach. Earth-Sci. Rev. 165, 151–184.

Chaumillon, E., Tessier, B., Reynaud, J.-Y., 2010. Stratigraphic records and variability of incised valleys and estuaries along French coasts. Bull. Société Géologique Fr. 181, 75–85.

Chotin, P., Brahim, L.A., 1988. Transpression et magmatisme au Néogène-Quaternaire dans le Maroc oriental. Comptes Rendus Académie Sci. Sér. 2 Mécanique Phys. Chim. Sci. Univers. Sci. Terre 306, 1479–1485.

Comas, M.C., Platt, J.P., Soto, J.I., Watts, A.B., 1999. 44. The origin and tectonic history of the Alboran Basin: insights from leg 161 results. In: Proceedings of the Ocean Drilling Program Scientific Results, pp. 555–580.

Costa, P.J.M., Gelfenbaum, G., Dawson, S., Selle, S.L., Milne, F., Cascalho, J., Lira, C.P., Andrade, C., Freitas, M.C., Jaffe, B., 2017. The application of microtextural and heavy mineral analysis to discriminate between storm and tsunami deposits. Geol. Soc. Lond. Spec. Publ. 456, SP456.7.

Das, O., Wang, Y., Donoghue, J., Xu, X., Coor, J., Elsner, J., Xu, Y., 2013. Reconstruction of paleostorms and paleoenvironment using geochemical proxies archived in the sediments of two coastal lakes in northwest Florida. Quat. Sci. Rev. 68, 142–153.

De Luca, P., 1978. L'unite chaotique des Kebdana (region de Zaio, Maroc). Relation structurale avec l'avant pays du Rif oriental. Bull. Société Géologique Fr. 7, 339–343.

Degeai, J.-P., Devillers, B., Dezileau, L., Oueslati, H., Bony, G., 2015. Major storm periods and climate forcing in the Western Mediterranean during the Late Holocene. Quat. Sci. Rev. 129, 37–56.

Dezileau, L., Sabatier, P., Blanchemanche, P., Joly, B., Swingedouw, D., Cassou, C., Castaings, J., Martinez, P., Von Grafenstein, U., 2011. Intense storm activity during the Little Ice Age on the French Mediterranean coast. Palaeogeogr. Palaeoclimatol. Palaeoecol. 299, 289–297.

Donnelly, J.P., Webb III, T., Murnane, R., Liu, K., 2004. Backbarrier sedimentary records of intense hurricane landfalls in the northeastern United States. Hurric. Typhoons Past Present Future 55, 58–95.

El Azzouzi, M'hammed, Bernard-Griffiths, J., Bellon, H., Maury, R.C., Piqué, A., Fourcade, S., Cotten, J., Hernandez, J., 1999. Évolution des sources du volcanisme marocain au cours du Néogène. C. R. Acad. Sci. Ser. IIA Earth Planet. Sci. 329, 95–102.

El Mrabet, T., 2005. The Great Earthquakes in the Maghreb Region and their Consequences on Man and Environment. CNRS-LAG, Rabat, Maroc (428 pp.).

Engel, M., Brückner, H., Wennrich, V., Scheffers, A., Kelletat, D., Vött, A., Schäbitz, F., Daut, G., Willershäuser, T., May, S.M., 2010. Coastal stratigraphies of eastern Bonaire (Netherlands Antilles): new insights into the palaeo-tsunami history of the southern Caribbean. Sediment. Geol. 231, 14–30.

Ferrarin, C., Bajo, M., Bellafiore, D., Cucco, A., De Pascalis, F., Ghezzo, M., Umgiesser, G., 2014. Toward homogenization of Mediterranean lagoons and their loss of hydro-diversity. Geophys. Res. Lett. 41, 5935–5941.

Ferrer, P., Benabdellouahed, M., Certain, R., Tessier, B., Barusseau, J.-P., Bouchette, F., 2010. The Late Holocene sediment infilling and beach barrier dynamics of the Thau lagoon (Gulf of Lions, Mediterranean Sea, SE France). Bull. Société Géologique Fr. 181, 197–209.

Goff, J., McFadgen, B.G., Chagué-Goff, C., 2004. Sedimentary differences between the 2002 Easter storm and the 15th-century Okoropunga tsunami, southeastern North Island, New Zealand. Mar. Geol. 204, 235–250.

Gomes, M., Humphries, M.S., Kirsten, K.L., Green, A.N., Finch, J.M., de Lecea, A.M., 2017. Diatom-inferred hydrological changes and Holocene geomorphic transitioning of Africa's largest estuarine system, Lake St Lucia. Estuar. Coast. Shelf Sci. 192, 170–180.

Gonzalez, M., Medina, R., Olabarrieta, M., Otero, L., 2010. Tsunami hazard assessment on the southern coast of Spain. Turk. J. Earth Sci. 19, 351–366.

Goslin, J., Clemmensen, L.B., 2017. Proxy records of Holocene storm events in coastal barrier systems: storm-wave induced markers. Quat. Sci. Rev. 174, 80–119.

Greene, H.G., Gardner-Taggart, J., Ledbetter, M.T., Barminski, R., Chase, T.E., Hicks, K.R., Baxter, C., 1991. Offshore and onshore liquefaction at Moss Landing spit, central California—result of the October 17, 1989, Loma Prieta earthquake. Geology 19, 945–949.

Guillemin, M., Houzay, J.-P., 1982. Le Néogène post-nappes et le Quaternaire du Rif nord-oriental; Stratigraphie et tectonique des bassins de Melilla, du Kert, de Boudinar et du piedmont des Kebdana. Editions du Service géologique du Maroc. (309 pp.).

Hamoumi, N., 2012. Le complexe lagunaire de Nador (Maroc): fonctionnement, contrôle naturel et provoqué, scenarii d'évolution future. Rev. Paralia 5, 5-1.

Irzi, Z., 1987. Etude sédimentologie et micropaléontologique de la lagune de Nador (Maroc oriental). Univ. Pièrre et Marrie Currie, Paris VI, Paris (160 pp.).

Irzi, Z., 2002. Les Environnements du Littoral méditerranéen du Maroc compris entre l'oued Kiss et le Cap des trois Fourches dynamique sédimentaire et évolution et écologie des foraminifères benthiques de la lagune de Nador. Univ. Mohammed Premier, Oujda (290 pp.).
Judd, K., Chagué-Goff, C., Goff, J., Gadd, P., Zawadzki, A., Fierro, D., 2017. Multi-proxy evidence for small historical tsunamis leaving little or no sedimentary record. Mar. Geol. 385, 204–215.
Kaabouben, F., Baptista, M.A., Iben Brahim, A., Mouraouah, A.E., Toto, A., 2009. On the Moroccan tsunami catalogue. Nat. Hazards Earth Syst. Sci. 9, 1227–1236.
Kakroodi, A.A., Kroonenberg, S.B., Hoogendoorn, R.M., Khani, H.M., Yamani, M., Ghassemi, M.R., Lahijani, H.A.K., 2012. Rapid Holocene sea-level changes along the Iranian Caspian coast. Quat. Int. 263, 93–103.
Khawfany, A.A., Aref, M.A., Taj, R.J., 2017. Human-induced changes in sedimentary facies and depositional environments, Sarum area, Red Sea coast, Saudi Arabia. Environ. Earth Sci. 76, 61.
Kelsey, H.M., Witter, R.C., Hemphill-Haley, E., 1998. Response of a small Oregon estuary to coseismic subsidence and postseismic uplift in the past 300 years. Geology 26, 231–234.
Lebret, N., 2014. Contexte structural et métallogénique des skarns à magnétite des Beni Bou Ifrour (Rif oriental, Maroc): apports à l'évolution géodynamique de la Méditerranée Occidentale. Univ. Orléans (470 pp.).
Leeper, R., Rhodes, B., Kirby, M., Scharer, K., Carlin, J., Hemphill-Haley, E., Avnaim-Katav, S., MacDonald, G., Starratt, S., Aranda, A., 2017. Evidence for coseismic subsidence events in a southern California coastal saltmarsh. Sci. Rep. 7.
Levy, Y., 1974. Sedimentary Reflection of Depositional Environment in the Bardawil Lagoon, Northern Sinai. J. Sediment. Res. 44, 210–227.
Liu, K., Fearn, M.L., 1993. Lake-sediment record of late Holocene hurricane activities from coastal Alabama. Geology 21, 793–796.
Louaya, A., Hamoumi, N., 2010. Etude morphostructurale de la région de Nador (Maroc nord-oriental). Afr. Géosciences Rev. 17, 107–127.
Luque, L., Lario, J., Zazo, C., Goy, J.L., Dabrio, C.J., Silva, P.G., 2001. Tsunami deposits as paleoseismic indicators: examples from the Spanish coast. Acta Geol. Hisp. 36, 197–211.
Mahjoubi, R., 2001. Nature et origine du flux de matières particulaires et son enregistrement dans un milieu paralique microtidal: cas de la lagune de Nador (Maroc nord oriental). Univ. Moulay Ismail, Meknès (231 pp.).
Matias, A., Ferreira, Ó., Vila-Concejo, A., Garcia, T., Dias, J.A., 2008. Classification of washover dynamics in barrier islands. Geomorphology 97, 655–674.
May, S.M., Vött, A., Brückner, H., Smedile, A., 2012. The Gyra washover fan in the Lefkada lagoon, NW Greece—possible evidence of the 365 AD Crete earthquake and tsunami. Earth Planets Space 64, 6.
Meghraoui, M., Morel, J.-L., Andrieux, J., Dahmani, M., 1996. Tectonique plio-quaternaire de la chaîne tello-rifaine et de la mer d'Alboran. Une zone complexe de convergence continent–continent. Bull. Soc. Geol. Fr. 167, 141–157.
Minoura, K., Nakaya, S., 1991. Traces of tsunami preserved in inter-tidal lacustrine and marsh deposits: some examples from northeast Japan. J. Geol. 99, 265–287.
Mitchum, R.M.J., Vail, P.R., Sangree, J.B., 1977. Seismic stratigraphy and global changes of sea level: part 6. Stratigraphic interpretation of seismic reflection patterns in depositional sequences: section 2. Application of seismic reflection configuration to stratigraphic interpretation. Seism. Stratigr. Appl. Hydrocarb. Explor. 165, 117–133.
Morel, J.-L., 1987. Évolution récente de l'orogène rifain et de son avant-pays depuis la fin de la mise en place des nappes (Rif, Maroc). Univ. Paris 11 (584 pp.).
Morel, J.L., 1989. Etats de contrainte et cinématique de la chaîne rifaine (Maroc) du Tortonien à l'actuel. Geodin. Acta 3, 283–294.
Morton, R.A., Gelfenbaum, G., Jaffe, B.E., 2007. Physical criteria for distinguishing sandy tsunami and storm deposits using modern examples. Sediment. Geol. 200, 184–207.
Nanayama, F., Shigeno, K., Satake, K., Shimokawa, K., Koitabashi, S., Miyasaka, S., Ishii, M., 2000. Sedimentary differences between the 1993 Hokkaido-nansei-oki tsunami and the 1959 Miyakojima typhoon at Taisei, southwestern Hokkaido, northern Japan. Sediment. Geol. 135, 255–264.
Nelson, A.R., Kelsey, H.M., Witter, R.C., 2006. Great earthquakes of variable magnitude at the Cascadia subduction zone. Quat. Res. 65, 354–365.
Nichol, S.L., Goff, J.R., Devoy, R.J.N., Chagué-Goff, C., Hayward, B., James, I., 2007. Lagoon subsidence and tsunami on the West Coast of New Zealand. Sediment. Geol. 200, 248–262.
Nieto, A.B., 1996. Cartografía histórica de Melilla (1497–1997). El Viso. ed, Quinto Centenario, Melilla (212 pp.).
Nieto-Moreno, V., Martínez-Ruiz, F., Giralt, S., Jiménez-Espejo, F., Gallego-Torres, D., Rodrigo-Gámiz, M., García-Orellana, J., Ortega-Huertas, M., de Lange, G.J., 2011. Tracking climate variability in the western Mediterranean during the Late Holocene: a multiproxy approach. Clim. Past 7, 1395–1414.
Nott, J., 2004. Palaeotempestology: the study of prehistoric tropical cyclones—a review and implications for hazard assessment. Environ. Int. 30, 433–447.
Palano, M., González, P.J., Fernández, J., 2013. Strain and stress fields along the Gibraltar Orogenic Arc: constraints on active geodynamics. Gondwana Res. 23, 1071–1088.
Pedoja, K., Djellit, H., Authemayou, C., Deverchere, J., Strzerzynski, P., Heddar, A., Nexer, M., Boudiaf, A., 2013. Comment on "active coastal thrusting and folding, and uplift rate of the Sahel anticline and Zemmouri earthquake area (Tell Atlas, Algeria)", by S. Maouche, M. Meghraoui, C. Morhange, S. Belabbes, Y. Bouhadad, H. Haddoum. [Tectonophysics, 2011, 509, 69–80]. Tectonophysics 601, 236–244.
Peláez, J.A., Chourak, M., Tadili, B.A., Brahim, L.A., Hamdache, M., Casado, C.L., Solares, J.M., 2007. A catalog of main Moroccan earthquakes from 1045 to 2005. Seismol. Res. Lett. 78, 614–621.
Poujol, A., Ritz, J.-F., Tahayt, A., Vernant, P., Condomines, M., Blard, P.-H., Billant, J., Vacher, L., Tibari, B., Hni, L., et al., 2014. Active tectonics of the Northern Rif (Morocco) from geomorphic and geochronological data. J. Geodyn. 77, 70–88.
Puga-Bernabéu, Á., Aguirre, J., 2017. Contrasting storm- versus tsunami-related shell beds in shallow-water ramps. Palaeogeogr. Palaeoclimatol. Palaeoecol. 471, 1–14.
Raji, O., Dezileau, L., Von Grafenstein, U., Niazi, S., Snoussi, M., Martinez, P., 2015. Sea extreme events during the last millennium in north-east of Morocco. Nat. Hazards Earth Syst. Sci. 15, 203–2011.
Raji, O., Niazi, S., Snoussi, M., Dezileau, L., Khouakhi, A., 2013. Vulnerability assessment of a lagoon to sea level rise and storm events: Nador lagoon (NE Morocco). J. Coast. Res. 65, 802–807.
Rampnoux, J.-P., Angelier, J., Colletta, B., Fudral, S., Guillemin, M., Pierre, G., 1977. Les resultats de l'analyse structurale et de la neotectonique des littoraux; B, les resultats de l'analyse structurale au Maroc. Bull. Société Géologique Fr. 7, 594–599.
Raynal, O., Bouchette, F., Certain, R., Sabatier, P., Lofi, J., Seranne, M., Dezileau, L., Briqueu, L., Ferrer, P., Courp, T., 2010. Holocene evolution of a Languedocian lagoonal environment controlled by inherited coastal morphology (northern Gulf of Lions, France). Bull. Société Géologique Fr. 181, 211–224.
Reicherter, K., Becker-Heidmann, P., 2009. Tsunami deposits in the western Mediterranean: remains of the 1522 Almería earthquake? Geol. Soc. Lond. Spec. Publ. 316, 217–235.
Reimer, P.J., Bard, E., Bayliss, A., Beck, J.W., Blackwell, P.G., Bronk Ramsey, C., Buck, C.E., Cheng, H., Edwards, R.L., Friedrich, M., et al., 2013. IntCal13 and Marine13 radiocarbon age calibration curves 0–50,000 years cal BP. Radiocarbon 55, 1869–1887.
Sabatier, P., Dezileau, L., Colin, C., Briqueu, L., Bouchette, F., Martinez, P., Siani, G., Raynal, O., Von Grafenstein, U., 2012. 7000 years of paleostorm activity in the NW Mediterranean Sea in response to Holocene climate events. Quat. Res. 77, 1–11.
Shah-hosseini, M., Morhange, C., Beni, A.N., Marriner, N., Lahijani, H., Hamzeh, M., Sabatier, F., 2011. Coastal boulders as evidence for high-energy waves on the Iranian coast of Makran. Mar. Geol. 290, 17–28.
Simpkin, P.G., Davis, A., 1993. For seismic profiling in very shallow water, a novel receiver. Sea Technol. U. S. 34 (9), 21–28 (Universite du Q.; University C. of N.W.).
Stefani, M., Vincenzi, S., 2005. The interplay of eustasy, climate and human activity in the Late Quaternary depositional evolution and sedimentary architecture of the Po Delta system. Mar. Geol. Mediterranean Prodelta Systems 222, 19–48.
Stich, Martin, Morales, 2007. Deformacion sismica y asismica en la zona Béticas-Rif-Alboran. Rev. Soc. Geol. Esp. 20, 311–319.
Stuiver, M., Reimer, P.J., 1993. Extended 14 C data base and revised CALIB 3.0 14 C age calibration program. Radiocarbon 35, 215–230.
Tosi, L., Rizzetto, F., Zecchin, M., Brancolini, G., Baradello, L., 2009. Morphostratigraphic framework of the Venice lagoon (Italy) by very shallow water VHRS surveys: evidence of radical changes triggered by human-induced river diversions. Geophys. Res. Lett. 36 (L09406), 1–5.
Tous, M., Romero, R., 2011. Medicanes: cataloguing criteria and exploration of meteorological environments. Tethys 8, 53–61.
Witter, R.C., Kelsey, H.M., Hemphill-Haley, E., 2001. Pacific storms, El Nino and tsunamis: competing mechanisms for sand deposition in a coastal marsh, Euchre Creek, Oregon. J. Coast. Res. 563–583.
Yahyaoui, A.M., Dakki, M., Hoepffner, C., Demnati, A., 1997. Le Bassin du Gareb-Bou Areg (Rif oriental): une région-clé pour l'interprétation de la structuration alpine de chaîne rifaine. Géologie Méditerranée 24, 73–92.
Zecchin, M., Tosi, L., Caffau, M., Baradello, L., Donnici, S., 2014. Sequence stratigraphic significance of tidal channel systems in a shallow lagoon (Venice, Italy). The Holocene 24, 646–658.
Zong, Y., Tooley, M.J., 1999. Evidence of mid-Holocene storm-surge deposits from Morecambe Bay, northwest England: a biostratigraphical approach. Quat. Int. 55, 43–50.